

# Distance-based Hyperspherical Classification for Multi-source Open-Set Domain Adaptation

Silvia Bucci\* Francesco Cappio Borlino\* Barbara Caputo Tatiana Tommasi  
Politecnico di Torino, Italy Italian Institute of Technology

{silvia.bucci, francesco.cappio, barbara.caputo, tatiana.tommasi}@polito.it

## Abstract

*Vision systems trained in closed-world scenarios will inevitably fail when presented with new environmental conditions, new data distributions and novel classes at deployment time. How to move towards open-world learning is a long standing research question, but the existing solutions mainly focus on specific aspects of the problem (single domain Open-Set, multi-domain Closed-Set), or propose complex strategies which combine multiple losses and manually tuned hyperparameters. In this work we tackle multi-source Open-Set domain adaptation by introducing HyMOS: a straightforward supervised model that exploits the power of contrastive learning and the properties of its hyperspherical feature space to correctly predict known labels on the target, while rejecting samples belonging to any unknown class. HyMOS includes a tailored data balancing to enforce cross-source alignment and introduces style transfer among the instance transformations of contrastive learning for source-target adaptation, avoiding the risk of negative transfer. Finally a self-training strategy refines the model without the need for handcrafted thresholds.*

*We validate our method over three challenging datasets and provide an extensive quantitative and qualitative experimental analysis. The obtained results show that HyMOS outperforms several Open-Set and universal domain adaptation approaches, defining the new state-of-the-art.*

## 1. Introduction

Artificial intelligent systems face a multitude of operational challenges when moving from the controlled lab environment to the real world. First of all the annotated data available to train a model might be the result of asynchronous multi-agent collection processes. For vision tasks this means dealing with datasets composed of labeled images that share the same class set, but with sub-groups of instances showing significant differences in appearance and

\*The authors equally contributed to this work.

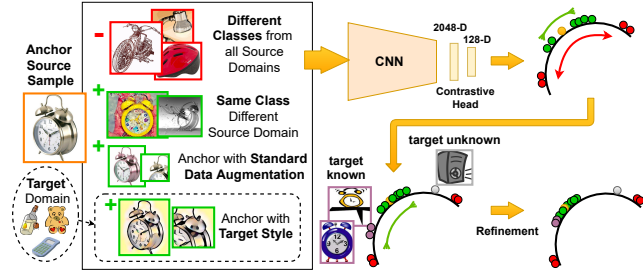


Figure 1: Schematic illustration of HyMOS. It learns a supervised contrastive model by balancing positive and negative pairs for each anchor sample over classes and domains, exploiting style transfer as an instance transformation process. Distance-based classification is applied on the learned hyperspherical feature space and is progressively refined via self-training.

style among each other. Moreover, at deployment time the learned model will inevitably encounter new environmental conditions, with distribution shift and novel classes not present during training. This complex scenario is attracting more and more attention in the computer vision community, with several studies on the sub-problems of domain adaptation and open-world learning which have been recomposed under the name of *Open-Set domain adaptation* [31]. In standard Closed-Set domain adaptation [7] the main focus is on how to reduce the gap between the training (labeled source) and test (unlabeled target) data when the latter is available since the beginning of the learning process and covers exactly the same class set of the former. Open-Set domain adaptation aims at bridging the domain gap while also rejecting target samples of unknown classes. Indeed, in case of category shift, the application of naïve adaptive solutions may lead to negative transfer and unrecoverable class misalignment. Although dealing with multiple sources is more the rule than an exception in real world conditions, only one recent work has started to peek into the multi-source Open-Set domain adaptation task [34]. This highlights the difficulty of learning a shared feature space for all the domains, while also maximizing the separation between

known and unknown categories within the unlabeled target.

The foundational problem that all the current open-world adaptive learning models try to solve is the limited generalization ability of the albeit powerful deep learning models. This can be at least partially explained considering two well known CNN shortcomings: (1) deep models yield features that describe mostly local rather than global statistics, which causes a bias on the image style of the training data [16]; (2) the cross-entropy loss, widely used for supervised learning, produces overconfident predictions thus biasing the model towards the labeled class set [17]. The existing strategies to avoid these issues usually adopt multi-stage learning procedures, combine several losses to compensate for the cross-entropy over reliance on source supervision and to close the domain gap with adversarial techniques. The obtained approaches are difficult to train with several hyperparameters to tune and manually-set thresholds. Moreover, the learning problem is often turned into a Closed-Set task by either synthetically generating negative instances for the source, or forcing the putative unknown samples into a single class, despite they actually belong to many different categories.

With our work we propose a supervised model that avoids the drawbacks of the cross-entropy loss, while learning an embedding space ready to accommodate new classes and new domains. **Specifically we show how the single supervised contrastive learning objective can tackle every challenge of multi-source Open-Set domain adaptation:**

- source to source class-wise alignment comes by simply balancing data batches over classes and domains;
- source to target adaptation is obtained by introducing style transfer as one of the data augmentation strategies in the typical double stream process of contrastive learning [5, 12, 17]. This solution also reduces the risk of cross-domain semantic misalignment generally due to the novel target categories.
- the separation between known and unknown target classes originates from the contrastive logic that creates compact class clusters with far centroids on the hyperspherical feature embedding [51]. Thus, the unknown categories naturally appear in low density regions.
- our distance-based classification model further benefits from a self-training procedure which does not need external hyper-parameters and is auto-regulated on the basis of the observed data distribution.

To highlight the important role of the **Hyperspherical** feature space for our **Multi-source Open-Set** approach, we dub it **HyMOS** (see Figure 1). Differently from its competitors, HyMOS relies on a single loss function and focuses on the known samples shared between source and target, progressively aligning them, while the unknown data are left isolated. We present an extensive experimental analysis

on three multi-source Open-Set datasets, showing how HyMOS outperforms current state-of-the-art methods. A thorough ablation study provides details on the internal functioning of the method.

## 2. Related works

**Domain Adaptation** A model trained and tested on data sharing the same label set but drawn from two different marginal distributions will inevitably show low performance. *Closed-Set domain adaptation* addresses this problem by increasing the invariance of the learned features over source and target domains. Several approaches focus on minimizing statistical metrics that reflect the distribution discrepancy [58, 24, 20]. Others rely on adversarial learning [10, 25, 44]. Recent strategies also exploit batch and feature normalization [3, 21, 57] as well as self-supervision [2, 56] to learn robust cross-domain embeddings. A different stream of works investigates how to reduce the domain shift directly at pixel level. They leverage on generative models which can transfer the style of the source to the target and vice-versa [35, 39, 11, 26]. When dealing with multiple sources, the extra challenge is in aligning all the domains among each other while producing a high discriminative feature space. Several source weighting techniques exploit knowledge graphs and feature transferability measures evaluated once or multiple times over training [32, 59, 49].

Considering that the target is unlabeled, being sure that its semantic content perfectly matches that of the source is unrealistic. *Open-Set domain adaptation* tackles target domains which include new unknown classes with respect to the source. After the definition of the problem in [31], a first group of works proposed various approaches to maximize the separation between known and unknown target samples while exploiting adversarial-based methods to align the known classes [38, 23, 8]. Most recently, [30] introduces a self-ensembling based method to minimize the model mismatch between the class assignment proposed by the source, and the inherent target cluster distribution. ROS [1] shows how to exploit the self-supervised rotation recognition task to deal with both these objectives. In [18] an *Inheritable* model is directly trained on the source with an extra set of negative samples produced via the suppression of class-specific feature maps activations.

The methods dealing with *universal domain adaptation* cover a wide range of scenarios with private classes in source and/or target, including the Open-Set. In DANCE [37] a neighborhood clustering technique is integrated with the standard cross-entropy loss to learn the structure of the target, while an entropy-based score is used to align or reject the target samples. In [9], CMU exploits a multi-classifier ensemble model together with an unknown scoring function which combines entropy, confidence and consistency

measures. The only published method dealing with multi-source Open-Set is MOSDANET [34] which adds a clustering objective over a standard supervised classification model to maximize the similarity among samples of the same class but different domains. Moreover, it exploits adversarial learning for domain adaptation: it has a tailored margin loss to penalize cases with a small difference in known and unknown prediction output, and finally it includes the potential target samples in the training procedure via pseudo-labeling.

**Contrastive Learning** Lately, self-supervised learning methods have shown that, by relying only on unlabeled data, it is still possible to get classification performance similar to those of the supervised approaches [42, 15, 5, 12]. Contrastive learning builds over instance discrimination techniques [54] (treating every instance as a class of its own), and aims at maximizing the agreement among multiple augmentations of the same sample, while pushing different instances far apart. Several methods have implemented this strategy by imposing the described constraints on the learned embedding space and they differ in how positive and negative data pairs are sampled and stored. Among the most cited, SimClr [5] adopts a large batch size, while MoCo [12] maintains a momentum encoder and a limited queue of previous samples. The effectiveness of the contrastive self-supervised learned embeddings is generally evaluated by using the pretext feature model as starting point for a downstream supervised task. However, more direct ways to incorporate supervision are currently attracting large attention [17, 52] and show how view invariance and semantic knowledge can be combined to get the best of both worlds in challenging scenarios as novelty detection [41], cross-domain generalization [61] or few-shot classification [27]. Current research is investigating ways to improve negative sampling [6], or present analyses to better understand the relation between contrastive learning and mutual information [53]. Some works have also studied the inherent properties of the contrastive loss function [47], proposing strategies to choose the best augmentation views [43, 33].

**Learning on the Unit Hypersphere** Fixed-norm representations have nice properties that support deep learning computational stability and their empirical success has been demonstrated over several tasks both within- and across-domains [55, 48, 57]. In particular, [29] shows how setting class prototypes a priori on the unit hypersphere allows to easily deal with open world problems. The uniform distribution of the data centers implies large margin separation among them and leaves space to include new categories while maintaining a highly discriminative embedding. A recent work has also highlighted how learning features uniformly distributed on the unit hypersphere with compact positive pairs is a crucial component of the success of contrastive learning [51].

Overall, the provided literature overview shows a clear path: contrastive learning can be used to learn a good normalized feature embedding, ready to generalize across domains and suitable to tackle the open world challenges.

### 3. Method

**Problem Formulation** In multi-source Open-Set domain adaptation we are given  $L$  labeled source domains  $\mathcal{S} = \{\mathcal{S}_1, \mathcal{S}_2, \dots, \mathcal{S}_L\}$ , where  $\mathcal{S}_i = \{\mathbf{x}_j^{s_i}, y_j^{s_i}\}_{j=1}^{N^{s_i}} \sim p_i$ , and one unlabeled target domain  $\mathcal{T} = \{\mathbf{x}_j^t\}_{j=1}^{N^t} \sim q$ , all drawn from different data distributions  $p_{i=1, \dots, L}, q$ . The sources share the same label set  $y^s \in \{1, \dots, \mathcal{C}_s\}$ , and it holds  $\mathcal{C}_s \subset \mathcal{C}_t$ , thus the target covers  $\mathcal{C}_{t \setminus s}$  additional classes which are considered *unknown*. Starting from this setup, the goal is to train a model on the source data, able to identify the label of each target sample, by either assigning it to one of the known  $|\mathcal{C}_s|$  classes, or rejecting it as unknown. Given the different relatedness levels of the target with each of the available sources, reducing the domain shift while avoiding the risk of negative transfer may be difficult, especially when the *openness*  $\mathbb{O} = 1 - \frac{|\mathcal{C}_s|}{|\mathcal{C}_t|}$  increases.

**Overview** To tackle the described task, we propose to leverage on the power of contrastive learning. Specifically we follow the double augmentation strategy of [5, 17], with the two transformed views of every input image propagated to the CNN encoder network. For each sample  $\{\mathbf{x}_k^s, y_k^s\}$  with  $k \in B = \{1, \dots, 2K\}$ , the features obtained via the encoder  $Enc(\mathbf{x}_k^s)$  enter the final contrastive head that further projects them to a normalized embedding, producing  $\mathbf{z}_k = Proj(Enc(\mathbf{x}_k^s))$ . On the obtained hyperspherical space the samples are compared among each other: the similarity between two augmented views of the same sample as well as between all the data pairs sharing the same label  $y_k^s$  is maximized, while the similarity of instances belonging to different classes is minimized. We indicate with  $\nu(k) = B \setminus \{k\}$  the double batch without the *anchor* sample of index  $k$ , and the positive pairs are  $\pi(k) = \{k' \in \nu(k) : y_{k'}^s = y_k^s\}$ . The supervised contrastive loss is [17]:

$$\mathcal{L}_{SupClr} = \sum_{k=1}^{2K} \frac{-1}{|\pi(k)|} \sum_{k' \in \pi(k)} \log \frac{\exp(\sigma(\mathbf{z}_k^s, \mathbf{z}_{k'}^s)/\tau)}{\sum_{n \in \nu(k)} \exp(\sigma(\mathbf{z}_k^s, \mathbf{z}_n^s)/\tau)}, \quad (1)$$

where  $\tau \in \mathbb{R}^+$  is the scalar temperature parameter, and  $\sigma(\cdot, \cdot)$  is the cosine similarity. With HyMOS we improve the generalization abilities of the contrastive model by (i) properly managing the data batches with the aim of getting the best *alignment among the available sources*; (ii) extending the adaptation to the target domain via *target style transfer* within the multi-view augmentation strategies; (iii) including an iterative *self-training* procedure based on the obtained data distribution on the hypersphere.

**Source-Source Alignment and Target Style Transfer** To

get a reliable multi-domain embedding, we start by reducing the gap among the source domains without decreasing the class discriminativeness. We set up the training batches by paying attention to both class and domain balancing. Each batch is evenly divided to cover all the  $|\mathcal{C}_s|$  classes, and for each class we select an equal number of samples from all the  $L$  source domains. The contrastive objective operating on this mixed set strengthens the cross-domain similarity within the same category, and maximizes the margin among different classes over all the domains. Still, the observed source distributions differ from that of the target and adapting to it is crucial to get reliable predictions.

With the goal of smartly avoiding the confusion induced by the presence of the unknown class in the target, we propose to rely on a pixel-based adaptive strategy able to manage the visual style of an image without involving its content. Indeed, the data augmentation at the basis of contrastive learning provides a natural way to include target-like source images in the training process. We exploit the instance normalization method AdaIN [14] to obtain style transferred images in an online fashion. At every iteration we decide with a probability  $r$  if each source image should be transformed by borrowing the style from a target image chosen randomly. Finally, the supervised contrastive loss will optimize a model invariant to the style transfer augmentation, exactly as it does for the other more standard instance augmentation strategies (*e.g.* color jittering, grayscale). Thus, we obtain features that rely less on the visual style coded in the image local statistics and gather more global shape information which is crucial for object recognition.

**Classification and Self-Training on the Hypersphere** The described learning procedure allows setting the feature space while training a source supervised model that produces large margins among well-clustered classes. When processing the target data and projecting them on the hyper-spherical embedding we expect them to mainly distribute in the low density regions among the source categories, with samples of known classes closer to the existing cluster centers than those of the unknown classes. This is the ideal condition to perform distance-based classification. Thus, differently from previous literature where the contrastive models are used as pretext and the projection head is dropped in favour of a standard cross-entropy loss, we propose to stay on the hypersphere while delivering the final prediction.

We define the prototype of each source class  $y^s$  by computing the corresponding feature average  $h_{y^s} = \frac{1}{N_{y^s}} \sum_{k \in y^s} z_k^s$ , re-projected on the unit hypersphere. For any target sample  $z^t$  we measure the cosine similarity to each source class prototype and we rescale it in  $[0, 1]$  to define the distance  $d_{h_{y^s}}(z^t) = \{1 - \sigma_{[0,1]}(z^t, h_{y^s})\}$  for  $y^s \in \{1, \dots, \mathcal{C}_s\}$ , which is used as confidence measure

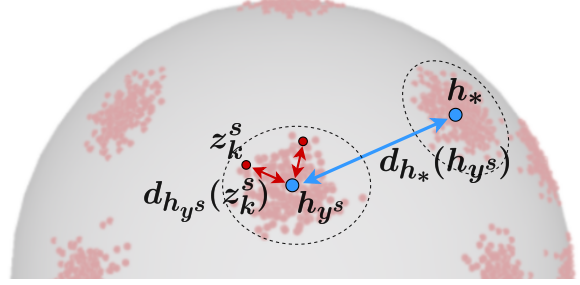


Figure 2: Illustration of the distances on the hypersphere used to set the class prediction and the self-training procedure.

for label assignment according to

$$\hat{y}^t = \begin{cases} \arg \min_{y^s} (d_{h_{y^s}}(z^t)) & \text{if } \min_{y^s} (d_{h_{y^s}}(z^t)) < \alpha \\ \text{unknown} & \text{if } \min_{y^s} (d_{h_{y^s}}(z^t)) \geq \alpha. \end{cases} \quad (2)$$

Here the threshold value  $\alpha$  is set on the basis of the observed data distribution. Specifically we introduce two metrics to evaluate it: the *class sparsity*

$$\theta = \frac{1}{|\mathcal{C}_s|} \sum_{y^s \in \mathcal{C}_s} d_{h_*}(h_{y^s}), \quad (3)$$

where  $h_*$  is the closest prototype to each  $h_{y^s}$ , and the *class compactness*

$$\phi = \frac{1}{|\mathcal{C}_s|} \sum_{y^s \in \mathcal{C}_s} \left\{ \frac{1}{N_{y^s}} \sum_{k \in y^s} d_{h_{y^s}}(z_k^s) \right\}. \quad (4)$$

In words, the former collects the prototype-to-prototype minimal distances and provides a measure of inter-class separation, while the latter evaluates whether the samples of each class are tight around the corresponding prototype (see Figure 2). A dataset with a large number of categories, each with small intra-class variability, results in a feature scenario with high compactness but low sparsity, for which a low threshold is needed. On the other extreme, a dataset with a limited number of categories showing large intra-class variability corresponds to a low compactness and high sparsity condition for which we can allow a higher threshold. We define the threshold as a multiple of the class compactness:

$$\alpha = \phi \cdot \left[ \log \left( \frac{\theta}{2\phi} \right) + 1 \right], \quad (5)$$

where  $\theta/2\phi$  estimates the average ratio between the distance of two adjacent prototypes and the radii of the respective clusters.

To further improve the source to target alignment and exploit the nature of the learned embedding, we go on learning by iteratively propagating the labels from the annotated

source samples to the unlabeled target data. We run a self-training procedure that focuses only on the samples recognized as known within a conservative threshold set as  $\alpha/2$ . The selected samples are progressively added to the training set, while unknown samples remain more and more isolated in empty regions of the feature space.

## 4. Implementation

We implemented HyMOS<sup>1</sup> with an architecture composed of the ResNet-50 [13] backbone and two fully connected layers of dimension 2048 and 128 which define the contrastive head. The overall network is trained by minimizing the contrastive loss (see Equation (1)), setting  $\tau = 0.07$  as in [41]. Our distance-based classifier lives in the final hyperspherical space produced by the model, and we can handle any final output dimensionality without being constrained to a specific number of classes. As a consequence, the architecture remains exactly the same for all our experiments.

We initialize the backbone network with the ImageNet pretrained SupClr model [17] and train HyMOS for 40k iterations with a balanced data mini-batch which contains one sample for each class of every source domain. The learning rate grows from 0 to 0.05 (at iteration 2500) with a linear warm-up schedule, to then decrease back to 0 at the end of training (iteration 40k) through a cosine annealing schedule. We use LARS optimizer [60] with momentum 0.9 and weight decay  $10^{-6}$ . For the first 20k iterations we train on source data only, using target data exclusively for the style transfer based data augmentation. We then perform an eval step in order to include confident known target samples in the learning objective. We repeat this eval step every 5K iterations till the end of the training.

For style transfer data augmentation we use the standard VGG19-based AdaIN model with default hyperparameters [14], trained with content data from the available source domains and target samples as style data.

For what concerns the instance transformations, we applied the same data augmentations originally proposed for SimClr [5], extending them with style transfer. Specifically, we used random resized crop with scale in  $\{0.08, 1\}$  and random horizontal flip. The style transfer is applied with probability  $r = 0.5$  on the source images, while the remaining not-stylized images are transformed via color jittering with probability  $p = 0.8$  and grayscale with probability  $p = 0.2$ .

## 5. Experiments

**Datasets** We evaluate our approach on three image classification benchmarks, following the same setting used in [34],

<sup>1</sup>The official Pytorch implementation of our method is available at <https://github.com/silvia1993/HyMOS>.

with one domain considered in turn as target. Office31 [36] comprises three domains: Webcam (W), Dslr (D) and Amazon (A) each containing 31 object categories. We set as known the first 20 classes in alphabetic order, while the remaining 11 are unknown. Office-Home [46] is made by four domains: Art (Ar), Clipart (Cl), Product (Pr), RealWorld (Rw) with 65 classes. The first 45 categories in alphabetic order are known, and the remaining 20 are unknown. DomainNet [32] is a more challenging testbed than the previous ones. It contains six domains and 345 classes. We considered Infograph (I), Painting (P), Sketch (S) and Clipart (C), selecting randomly 50 samples per class or using all the images in case of lower cardinality. The first 100 classes in alphabetic order are known, while the remaining 245 are unknown.

**Results** We assess the performance of HyMOS by comparing it with several state-of-the-art baselines proposed for single-source Open-Set (Inheritable [18], ROS [1]), multi-source Open-Set (MOSDANET [34]) and universal domain adaptation (CMU [9], DANCE [37]). We use the code provided by the authors<sup>2</sup>, and for all the methods that do not specify how to manage multiple sources we apply the *Source Combine* strategy [32] that considers the union of all the source data in a single domain.

We evaluate the following metrics: the average class accuracy over the known classes  $OS^*$ , the accuracy over the unknown class  $UNK$  and their harmonic mean  $HOS = \frac{2 \cdot OS^* \times UNK}{OS^* + UNK}$ . In the following we mainly focus on the last to discuss the results: as stated in [1, 9],  $HOS$  is fair indicator of how the used classification algorithms perform on both known and unknown samples.

Table 5 collects the result over the three considered datasets showing how HyMOS outperforms all the baselines with a gain in  $HOS$  from 1.9% up to 10.8% with respect to the best competitor ROS. The method Inheritable is better able to identify the unknown samples rather than annotating the known ones, resulting in a low  $HOS$  accuracy. On the other way round, both the universal approaches CMU and DANCE show high  $OS^*$ , but they poorly recognize the unknown samples. Only CMU on Office-Home has a good  $UNK$  value, but its  $HOS$  remains lower than that of ROS and of HyMOS. Finally, we highlight how the advantage of HyMOS is particularly visible on DomainNet where the classification task is extremely tough due to the high number of classes and the broad shift among the domains.

Figure 3 provides an overview on the behaviour of the dynamic threshold  $\alpha$  as well as of the  $HOS$  performance at different training iterations for all the three considered datasets. It is interesting to notice how  $\alpha$  differs in each case, both in terms of magnitude and trend: for Office31

<sup>2</sup>For all the baseline methods the implementations are publicly available, with the only exception of MOSDANET [34] for which we obtained the code via private communications with the authors.

Office31													DomainNet									
	D,A → W			W,A → D			W,D → A			Avg.			I,P → S			I,P → C			Avg.			
	OS*	UNK	HOS	OS*	UNK	HOS	OS*	UNK	HOS	OS*	UNK	HOS	OS*	UNK	HOS	OS*	UNK	HOS	OS*	UNK	HOS	
Source Combine	Inheritable [18]	68.1	87.6	76.6	74.1	85.6	79.5	62.9	78.9	70.0	68.4	84.0	75.4	24.5	60.3	34.8	33.1	65.6	44.0	28.8	62.9	39.4
	ROS [1]	82.3	81.5	81.8	96.5	68.7	80.1	52.2	84.9	64.7	77.0	78.4	75.5	31.3	77.5	44.5	40.7	73.6	52.4	36.0	75.5	48.5
	CMU [9]	98.7	44.6	61.4	98.7	47.3	64.0	74.5	45.4	56.4	90.6	45.8	60.6	48.3	26.3	38.1	49.8	27.6	35.5	49.1	27.0	36.8
	DANCE [37]	99.5	23.9	38.5	100.0	42.6	59.7	79.6	45.6	58.0	93.0	37.3	52.0	45.8	22.3	30.0	54.7	28.7	37.6	50.3	25.5	33.8
Multi-Source	MOSDANET [34]	99.4	43.5	60.5	99.0	55.9	71.5	81.5	67.6	73.9	93.3	55.7	68.6	29.9	60.2	40.0	31.6	51.8	39.3	30.8	56.0	39.6
	HyMOS	96.3	83.8	89.6	97.3	82.8	89.5	48.1	82.4	60.8	80.6	83.0	79.9	43.2	86.0	57.5	47.4	85.5	61.0	45.3	85.8	59.3

Office-Home																
	Ar,Pr,Cl → Rw			Ar,Pr,Rw → Cl			Cl,Pr,Rw → Ar			Cl,Ar,Rw → Pr			Avg.			
	OS*	UNK	HOS	OS*	UNK	HOS	OS*	UNK	HOS	OS*	UNK	HOS	OS*	UNK	HOS	
Source Combine	Inheritable [18]	58.4	68.9	63.2	43.7	66.5	52.6	35.5	77.6	48.7	58.5	63.3	60.7	49.1	69.1	56.3
	ROS [1]	69.8	76.9	<b>73.0</b>	57.1	57.6	57.3	57.2	66.7	61.6	70.3	68.0	69.1	63.6	67.3	65.3
	CMU [9]	62.5	81.5	70.8	34.6	89.9	50.0	43.7	87.0	58.1	60.1	81.7	69.3	50.2	85.0	62.1
	DANCE [37]	85.6	4.5	12.4	68.0	9.2	16.1	74.1	10.7	18.6	86.7	13.4	22.9	78.6	9.4	17.5
Multi-Source	MOSDANET [34]	79.4	55.0	65.0	68.1	40.9	51.1	61.3	48.7	54.3	82.2	55.0	65.9	72.8	49.9	59.1
	HyMOS	69.4	72.7	71.0	51.7	86.0	<b>64.6</b>	49.4	84.1	<b>62.2</b>	71.5	70.6	<b>71.1</b>	60.5	78.4	<b>67.2</b>

Table 1: Accuracy (%) averaged over three runs for each method on the Office31, DomainNet and Office-Home datasets.

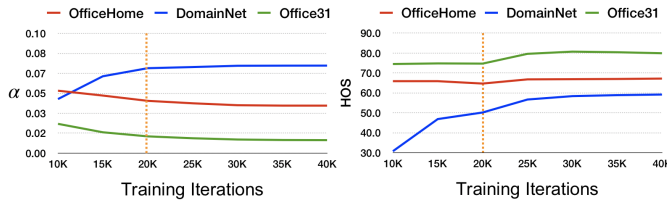


Figure 3: Analysis on the dynamic threshold  $\alpha$  (left) and of the recognition accuracy  $HOS$  (right) at different training iterations. The dotted line at 20k indicates the self-training starting point.

and Office-Home the threshold decreases over time while for DomainNet it increases. These variations reflect how the data clusters move: as the training proceeds they become more compact and the reciprocal distance increases towards a more uniform class distribution on the hypersphere. For DomainNet the second event occurs faster than the first: this behaviour is correlated with the class number/population which is higher/lower with respect to that of the other datasets. In all the cases, the threshold converges to a stable value.

For what concerns the performance of the model, we observe an almost fix (Office-Home, Office31) or growing (DomainNet) trend at the beginning of the learning process, with a noticeable improvement after the activation of the self-training procedure.

To conclude, we add a remark on the use of self-training. This procedure is often considered risky due to the possible wrongly annotated samples that can cause a drift in the model. To avoid this issue, several works have opted in favour of consistency regularization methods [40]. Still, the most recent literature has confirmed the effectiveness and safe nature of self-training when the sample selection criterion is chosen with a self-pacing strategy based on the distribution of the unlabeled samples [4], exactly as done by HyMOS.

## 6. Delving into the Details

With respect to the state-of-the-art Open-Set methods that rely on multi-stage approaches and combine several losses, HyMOS is much simpler. We designed it to be straightforward but also keeping in mind all the specific challenges of multi-source Open-Set domain adaptation. In the following we focus on each of them to shed light on the inner functioning of our method.

**Source-Source Alignment** Reducing the domain shift among the available sources helps to get models better able to generalize. This aspect is largely discussed in multi-source Closed-Set domain adaptation literature [59, 49]. A dedicated source alignment component is also included in the only existing multi-source Open-Set method MOSDANET.

HyMOS obtains cross-source adaptation thanks to the batch sampling strategy adopted to maintain a fair source balance during the learning process. Each mini-batch in training contains one sample for each class and for each domain. The supervised contrastive loss seamlessly does the rest by pulling together samples of same class (but different domains) and pushing away samples of different classes (regardless of the domain). If we turn off the sample balancing we experience a drop in performance of about 2.6% as shown by *HyMOS No Source Balancing* in Table 2.

**Source-Target Adaptation** In the Open-Set scenario the naïve application of any feature-based domain adaptation strategy over source and target may be detrimental due to the presence of the extra unknown target category. HyMOS performs cross-domain adaptation avoiding negative transfer both via pixel-based adaptation and with self-training only on the known classes.

The use of style-transfer as one of the data transformations at the basis of contrastive learning helps the model to focus on domain invariant visual characteristics without involving the target data semantic content. To evaluate more precisely the effect of this approach we present two abla-

Office-Home															
	Ar,Pr,Cl → Rw			Ar,Pr,Rw → Cl			Cl,Pr,Rw → Ar			Cl,Ar,Rw → Pr			Avg.		
	OS*	UNK	HOS	OS*	UNK	HOS									
<b>HyMOS</b>	69.4	72.7	71.0	51.7	86.0	64.6	49.4	84.1	62.2	71.5	70.6	71.1	60.5	78.4	<b>67.2</b>
HyMOS No Source Balance	61.7	78.7	69.2	44.1	86.5	58.4	47.1	85.0	60.6	70.3	70.1	70.2	55.8	80.1	64.6
HyMOS Style Tr. Only Known Target	70.6	70.8	70.7	50.7	85.8	63.7	49.4	85.0	62.5	71.6	70.8	71.2	60.6	78.1	67.0
HyMOS No Style Transfer	66.4	72.9	69.5	41.7	87.5	56.4	47.6	80.9	60.0	71.3	65.6	68.3	56.7	76.7	63.6
HyMOS No Self-Training	64.5	82.0	72.2	39.4	91.0	55.0	43.5	90.0	58.6	63.3	82.3	71.5	52.7	86.3	64.3
HyMOS Source Only	58.1	86.0	69.4	28.8	93.6	44.0	38.3	89.0	53.6	59.6	82.7	69.3	46.2	87.8	59.1
Improved Cross-Entropy Baseline	71.2	54.1	61.5	59.6	62.9	61.2	53.2	64.1	58.1	72.5	47.1	57.1	64.1	57.1	59.5

Table 2: Ablation Study.

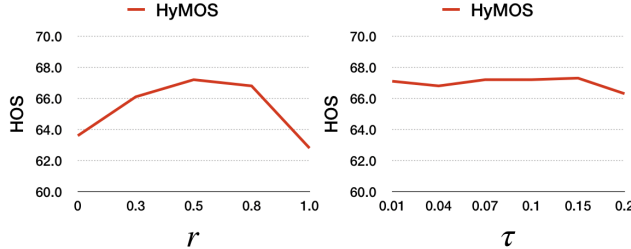


Figure 4: Sensitivity analysis for the two HyMOS hyperparameters on Office-Home: (left) the style transfer probability  $r$  and (right) the temperature value  $\tau$ .

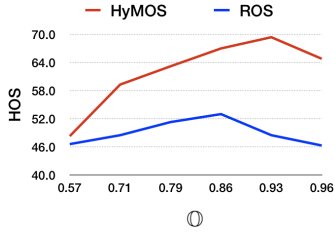


Figure 5: Performance comparison between HyMOS and ROS [1] at different openness ( $\odot$ ) levels on DomainNet.

tion cases: the first considers an oracle which extracts the reference style only from target samples of known classes (*HyMOS Style Tr. Only Known Target*), while the second turns off completely the style transfer augmentation (*HyMOS No Style Transfer*). As clear from the obtained results in Table 2, the style transfer is class agnostic and the presence or absence of the unknown class in the target does not affect the performance. On the other hand, using or not the style transfer makes a significant difference: the obtained *HOS* without style transfer remains competitive with respect to the other baselines, but drops of about 3.6% below the complete version of HyMOS.

Also the self-training procedure has a relevant role in the final performance: by checking the prediction output before the first group of target data is included in the training set (*HyMOS No Self-Training*) we observe a decrease of 2.9% in *HOS*. Finally, disabling both style transfer and self-training (*HyMOS Source Only*) prevents source-target adaptation causing a significant result drop of about 8%.

### Comparison with an Improved Cross-Entropy Baseline

Source balancing, style transfer and self-training appear as simple strategies that can be integrated in any supervised learning model to improve its effectiveness in the multi-source Open-Set scenario. Still, we state that leveraging on supervised contrastive learning and its related hyperspherical feature embedding is crucial for the task at hand. To support our claim we ran an experimental test by substituting the contrastive loss of HyMOS with standard cross-entropy, while keeping the same original side strategies: domain balance in the training mini-batches, augmentation of the source via style transfer from the target, and self-training. The last one operates by progressively including confident pseudo-labeled known target samples in the training with a threshold on prediction output analogous to that proposed in [34]. The last row of Table 2 reports the obtained results, showing that this baseline approach, despite the included adaptive strategies, performs just slightly better than *HyMOS Source Only* and it is significantly worse than HyMOS.

**Robustness to Hyperparameter Variation** HyMOS has two main hyperparameters: the style transfer probability  $r$  and the temperature  $\tau$  of the contrastive loss. The first controls which fraction of the source instances are augmented via style transfer. Setting  $r = 0$  means turning off style transfer, while  $r = 1$  means that style transfer overrules other more standard transformations while training the contrastive model. As shown in the left plot of Figure 4 both these extremes are not ideal choices, while values in  $\{0.3, 0.5, 0.8\}$  produce a small variation in the HyMOS results that remain always higher than that of the best competitor ROS (65.3).

The parameter  $\tau$  has an important role in the contrastive learning objective as discussed in [47]: it influences both the uniformity of sample distribution on the hypersphere and the weight given to hard positive/negative samples. We followed previous literature in setting a low temperature value [17], and we evaluate here the effect of tuning it. The right plot in Figure 4 confirms that with values lower than 0.1 the results remain stable (and always higher than ROS, 65.3), while moving towards 0.2 may cause a decrease in performance.

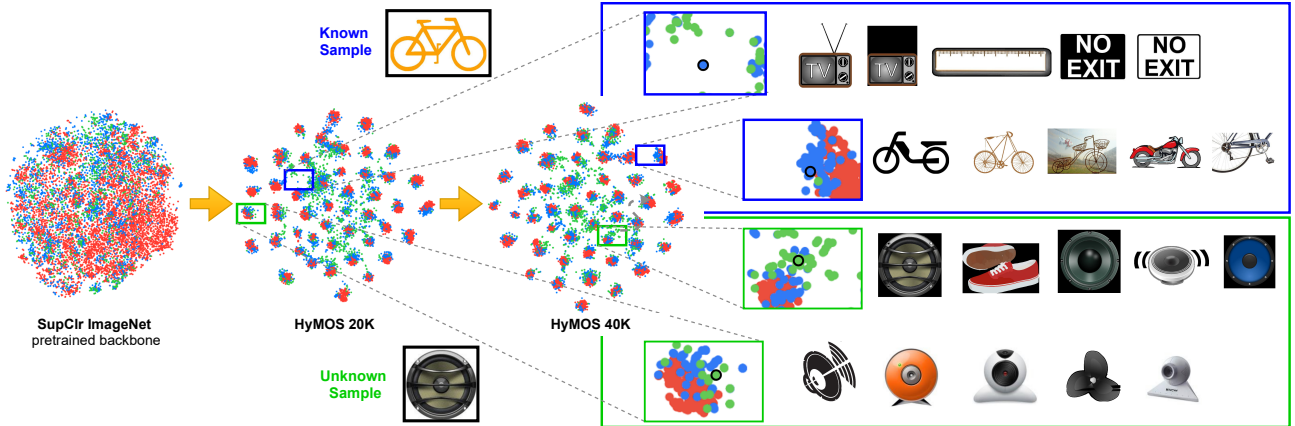


Figure 6: Qualitative analysis on the Ar,Pr,Rw → Cl case of the Office-Home dataset. The red dots represent the source domain, the blue dots are the known samples of the target domain and the green dots the unknown ones. HyMOS 20k: source balancing and style transfer already favour a good alignment of most of the known target classes with the respective source known cluster. HyMOS 40k: self-training further move the target known samples towards the respective source clusters, while the unknown samples remain in the regions among the clusters. The zooms show how the neighborhood of a known (bike) and unknown (speaker) target samples change during training.

**Increasing the Openness Level** In real world conditions it is difficult to have a direct control on the number of unknown classes in the unlabeled target, and it is natural to expect more unknown categories than known ones. To extensively study the behavior of HyMOS at different openness levels we consider the DomainNet dataset and exploit its large class cardinality. The plot in Figure 5 shows the performance of HyMOS and how it outperforms its best competitor ROS at different openness values  $\mathbb{O} \in \{0.5, 1\}$ .

## 7. Qualitative Analysis

We visualize the distribution of source and target data in the feature space (output of the contrastive head) with the t-sne [45] plots in Figure 6. In particular we focus on the Ar,Pr,Rw → Cl case of the Office-Home dataset: the red dots represent the source domain, the blue dots are the known samples of the target domain and the green dots the unknown ones. We take three snapshots of the data on the hyperspherical embedding: at the beginning when the backbone network is inherited from SupCir [17] pretrained on ImageNet, immediately before the application of self-training, and at the end of the training process. By observing the intermediate plot we can state that source balancing and style transfer already favour a good alignment of most of the known (blue) target classes with the respective source known clusters (red). The last plot indicates that self-training further improves the alignment while the unknown samples (green) remain in the regions among the clusters.

Randomly zooming on a known sample (the bike) and on an unknown sample (the speaker) we observe how their position change during training. The first moves from an

isolated region where its top five neighbours show high class confusion, towards the correct bike class. The second starts from a neighborhood populated by several samples of classes webcam and fan, and finally moves to a different region shared mostly by other instances of the class speaker.

## 8. Conclusions

In this paper we introduced HyMOS, a straightforward approach for multi-source Open-Set domain adaptation. It exploits contrastive learning and the inherent properties of its hyperspherical feature space to avoid the limitations of the existing competing methods. HyMOS includes a tailored data balancing to enforce cross-source alignment and introduces style transfer among the instance transformations for source-target adaptation, keeping away from the risk of negative transfer. Finally a self-training strategy refines the model without the need of manually set thresholds. Through extensive experiments we demonstrated state-of-the-art results on three benchmarks and we delved into the details of the methods with several quantitative and qualitative evaluations which shed light on its internal functioning.

We believe that the effectiveness of contrastive learning could be further leveraged for future extensions of HyMOS to the universal and class-incremental domain adaptation [19] settings, towards real-world life-long learning.

**Acknowledgements.** This work was partially supported by the ERC project RoboExNovo. Computational resources were provided by IIT (HPC infrastructure) and HPC@PoliTo. We also thank Biplab Banerjee for the insightful discussions on MOSDANET [34] while running this baseline.

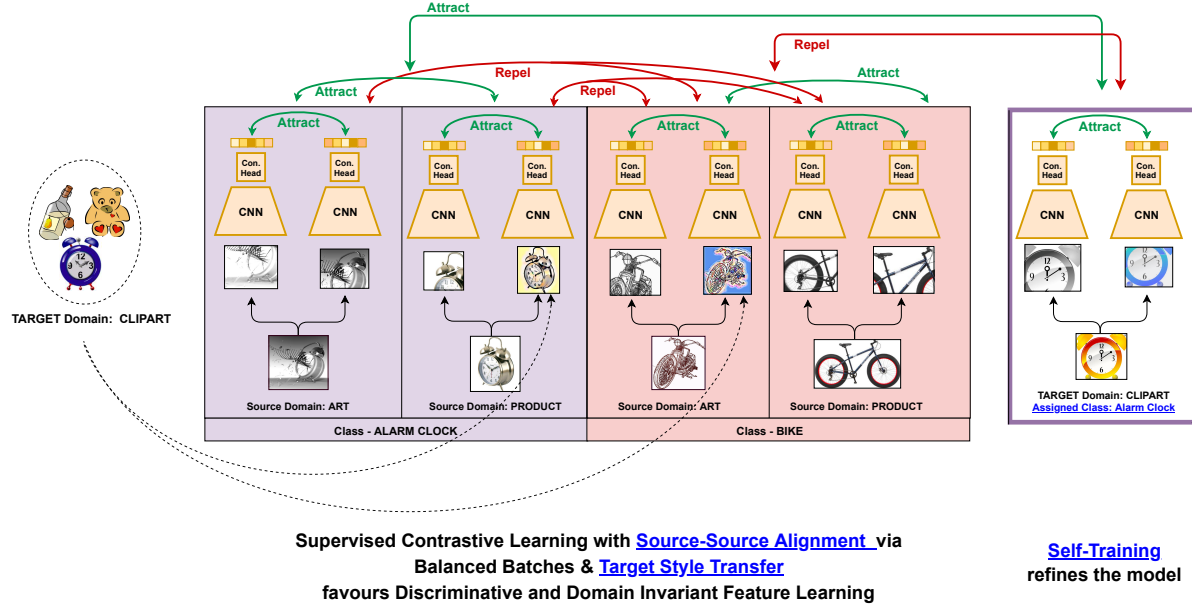


Figure 7: Schematic overview of HyMOS showing how the contrastive attraction/repulsion actions are applied among samples of different classes and domains.

## Appendix

### A. Contrastive learning in HyMOS

We include in Figure 7 a scheme explaining how contrastive learning works in our model together with source balancing, style transfer and self-training.

### B. Analysis on threshold multiplier

In HyMOS we designed a self-paced procedure which learns the threshold  $\alpha$  (to separate known/unknown target samples) from data distribution, over the whole training. The  $\alpha_m=0.5$  multiplier of  $\alpha$  indicated at the end of Section 3 is our only real hyperparameter: by modifying it one could decide at training time to favor recognition of known classes ( $OS^*$ ) at the expense of a lower  $UNK$ . The results in Table 3 show that  $\alpha_m=0.5$  is a safe choice regardless of the dataset. Moreover, by tuning this multiplier the  $HOS$  performance of HyMOS remains always higher than that of the best competitor ROS, and can even increase as in the case of DomainNet for  $\alpha_m=1$ .

### C. Further experiments

**Comparison with an improved version of ROS [1]** The self-supervised based method ROS has shown to be our best competitor over all the experimental tests conducted in the main paper. Here we discuss its behaviour when combined with the three strategies included in HyMOS: source balancing, style transfer and self-training.

	Office-Home (Avg.)			DomainNet (Avg.)		
$\alpha_m$	$OS^*$	UNK	$HOS$	$OS^*$	UNK	$HOS$
HyMOS	0.3	57.1	80.9	65.8	39.7	89.9
	0.5	60.5	78.4	67.2	45.3	85.8
	0.7	61.7	75.6	66.8	47.9	83.4
	1.0	65.6	68.0	65.8	50.2	79.0
ROS [1]	63.6	67.3	65.3	36.0	75.5	48.5

Table 3: Average performance on Office-Home and DomainNet when changing the multiplier  $\alpha_m$  to the self-paced threshold  $\alpha$ .

The results in the third row of Table 4 indicate that organizing the training data batches so that they contain a balanced set of source domains does not provide an improvement with respect to the standard version of ROS. The source-to-source alignment visible for HyMOS does not appear here: indeed feeding all the data at once to a learning model guided by the cross-entropy loss does not induce the same inherent clustering and adaptation effect that can be obtained via contrastive learning.

The fourth row shows the effect of using style transfer as data augmentation in ROS. Despite the advantage in  $OS^*$ , we observe a significant decrease in  $UNK$ , which indicates how this strategy may generate confusion in the considered Open-Set scenario. As already discussed in the main paper, we claim that introducing style transfer within the contrastive model is the right way to favour adaptation without suffering from negative transfer.

		Office-Home												Avg.						
		Ar,Pr,Cl → Rw				Ar,Pr,Rw → Cl				Cl,Pr,Rw → Ar				Cl,Ar,Rw → Pr				Avg.		
		OS*	UNK	HOS	OS*	UNK	HOS	OS*	UNK	HOS	OS*	UNK	HOS	OS*	UNK	HOS	OS*	UNK	HOS	
<b>HyMOS</b>		69.4	72.7	71.0	51.7	86.0	64.6	49.4	84.1	62.2	71.5	70.6	71.1	60.5	78.4	<b>67.2</b>				
ROS [1]		69.8	76.9	73.0	57.1	57.6	57.3	57.2	66.7	61.6	70.3	68.0	69.1	63.6	67.3	65.3				
ROS [1] + Source Balance		71.3	79.5	75.2	56.2	54.8	55.5	57.3	69.1	62.6	70.2	64.0	66.9	63.7	66.8	65.0				
ROS [1] + Style Transfer		73.9	54.4	62.6	67.0	35.4	46.3	57.8	47.2	52.0	73.9	50.8	60.1	68.2	46.9	55.2				
ROS [1] + Self-Training		71.2	68.0	69.6	58.1	60.2	59.1	55.8	68.6	61.5	74.2	51.1	60.5	64.8	62.0	62.7				
ROS [1] + S. Balance, Style Tr., Self-Train.		77.1	51.9	62.0	67.0	28.9	40.4	59.5	46.5	52.2	71.2	55.6	62.4	68.7	45.7	54.3				

Table 4: Improved version of ROS [1].

		Office31												DomainNet															
		D,A → W				W,A → D				W,D → A				Avg.				LP → S				LP → C				Avg.			
		OS	OS*	UNK	HOS	OS	OS*	UNK	HOS	OS	OS*	UNK	HOS	OS	OS*	UNK	HOS	OS	OS*	UNK	HOS	OS	OS*	UNK	HOS	OS	OS*	UNK	HOS
Source Combine	Inheritable [18]	69.0	68.1	87.6	76.6	74.7	74.1	85.6	79.5	63.7	62.9	78.9	70.0	69.1	68.4	84.0	75.4	24.9	24.5	60.3	34.8	33.5	33.1	65.6	44.0	29.2	28.8	62.9	39.4
Source Combine	ROS [1]	82.2	82.3	81.5	81.8	95.3	96.5	68.7	80.1	53.8	52.2	84.9	64.7	77.1	77.0	78.4	75.5	31.7	31.3	77.5	44.5	41.0	40.7	73.6	52.4	36.4	36.0	75.5	48.5
Source Combine	CMU [9]	96.1	98.7	44.6	61.4	96.2	98.7	47.3	64.0	73.1	74.5	45.4	56.4	88.5	90.6	45.8	60.6	48.0	48.3	26.3	38.1	49.6	49.8	27.6	35.5	48.8	49.1	27.0	36.8
Source Combine	DANCE [37]	95.9	99.5	23.9	38.5	97.3	100.0	42.6	59.7	78.0	79.6	45.6	58.0	90.4	93.0	37.3	52.0	45.6	45.8	22.3	30.0	54.4	54.7	28.7	37.6	50.0	50.3	25.5	33.8
Multi-Source	MOSDANET [34]	97.7	99.4	43.5	60.5	97.0	99.0	55.9	71.5	80.9	81.5	67.6	<b>73.9</b>	91.9	93.3	55.7	68.6	30.2	29.9	60.2	40.0	31.8	31.6	51.8	39.3	31.0	30.8	56.0	39.6
Multi-Source	<b>HyMOS</b>	95.7	96.3	83.8	<b>89.6</b>	96.6	97.3	82.8	<b>89.5</b>	49.8	48.1	82.4	60.8	80.7	80.6	83.0	<b>79.9</b>	43.6	43.2	86.0	<b>57.5</b>	47.8	47.4	85.5	<b>61.0</b>	45.7	45.3	85.8	<b>59.3</b>

		Office-Home												Office31												Avg.											
		Ar,Pr,Cl → Rw				Ar,Pr,Rw → Cl				Cl,Pr,Rw → Ar				Cl,Ar,Rw → Pr				Avg.				D,A → W				W,A → D				W,D → A				Avg.			
		OS	OS*	UNK	HOS	OS	OS*	UNK	HOS	OS	OS*	UNK	HOS	OS	OS*	UNK	HOS	OS	OS*	UNK	HOS	OS	OS*	UNK	HOS	OS	OS*	UNK	HOS	OS	OS*	UNK	HOS				
ROS [1]		68.0	63.9	66.0		80.8				69.6		73.7		79.4		75.9		93.9		95.2		73.5		<b>87.5</b>													
<b>HyMOS</b>		75.7	71.3	<b>73.5</b>		80.1				75.8		73.7		77.4		<b>76.7</b>		95.3		93.8		70.7		86.6													

Table 5: Accuracy (%) averaged over three runs for each method on the Office31, DomainNet and Office-Home datasets.

		DomainNet												Office-Home												Avg.								
		I,P → S				I,P → C				Avg.				Ar,Pr,Cl → Rw				Ar,Pr,Rw → Cl				Cl,Pr,Rw → Ar				Cl,Ar,Rw → Pr				Avg.				
		OS	OS*	UNK	HOS	OS	OS*	UNK	HOS	OS	OS*	UNK	HOS	OS	OS*	UNK	HOS	OS	OS*	UNK	HOS	OS	OS*	UNK	HOS	OS	OS*	UNK	HOS					
ROS [1]		68.0	63.9	66.0		80.8				69.6		73.7		79.4		75.9		93.9		95.2		73.5		<b>87.5</b>										
<b>HyMOS</b>		75.7	71.3	<b>73.5</b>		80.1				75.8		73.7		77.4		<b>76.7</b>		95.3		93.8		70.7		86.6										

Table 6: AUROC.

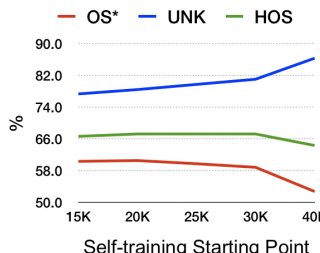


Figure 8: Analysis on the self-training starting point on Office-Home. The training ends at 40k: the results show that our model is overall robust to the specific choice of the self-training starting point, but moving it to the very latest phase of the learning procedure is detrimental.

We also followed [34] to extend ROS with self-training. The values of  $OS^*$  and  $UNK$  show respectively a relative improvement and decrease, resulting in a lower  $HOS$ . This confirms how self-training may be detrimental if not properly defined and used. Finally, when applying all the strategies at once, the results are similar to those obtained with style transfer alone: this last technique clearly steered the whole method towards a low performance.

**Analysis on the self-training starting point** To further investigate the role of self-training in HyMOS we studied the

effect of anticipating or delaying the inclusion of pseudo-labeled target data in the learning objective. All the experiments in the main paper were done by setting the self-training start point at 20K iterations. Here we move it in  $\{15K, 20K, 25K, 30K\}$ , while for the subsequent evaluation and model update steps we keep the original strategy performing them every 5K iterations after the first one. The obtained results are shown in Figure 8 and also include the case of turning off self-training with the first evaluation step at the end of the training process 40K. From the plot we see that  $HOS$  remains stable for all the configurations before 40K, while a late inclusion of the target favors  $UNK$  and decreases  $OS^*$ . This behaviour should be clearly avoided and highlights how the alignment effect of the contrastive objective on the shared classes of source and target declines if applied too late: the attracting force applied on the target samples towards the corresponding source clusters is largely reduced.

**Complete results with additional metrics** For completeness in Table 5 we present the same results of the main paper including also the  $OS$  metric, defined as  $OS = \frac{|\mathcal{C}_s|}{|\mathcal{C}_s|+1} \times OS^* + \frac{1}{|\mathcal{C}_s|+1} \times UNK$ .

In order to better understand HyMOS ability to separate known and unknown samples we also computed the AU-

ROC (Area Under the Receiver Operating Characteristic Curve) and performed a comparison with our strongest competitor ROS [1] in Table 6. The ROC curve is a graph plotting the true positive rate against the false positive rate by all possible values of the separating threshold. Therefore the area under this curve provides a threshold-free metric to understand the performance of a normality score and is often used to compare anomaly detection methods [41, 28]. In our case the normality score computed for target samples is the distance from known class centroids.

HyMOS results are comparable with those of ROS for Office-Home and Office31 and remarkably better for DomainNet, once again proving the good performance of HyMOS on large scale datasets. In any case the better HOS performance of HyMOS w.r.t the competitors even when the AUROC is comparable means that our method has an higher adaptation ability.

**Extension to Closed-Set and Universal settings.** HyMOS can be easily extended to the simpler multi-source Closed-Set DA setting (perfect overlap between sources and target classes) and to the more challenging multi-source Universal DA setting (both sources and target have their own private categories). For a preliminary evaluation on these scenarios we consider the DomainNet dataset. In the universal setting we follow [9] considering, in the alphabet order, the first 150 classes as shared between sources and target, the next 50 categories as sources private classes and the rest as target private classes; for the Closed-Set scenario we follow [22]. In Table 7 (top part), we compare against LtC-MSDA [50] and the very recent DRT [22]. The first one explores interactions among domains learning a graph with the domains prototypes to exploit the information propagation among semantically adjacent representations. The second one proposes to adapt the model parameters across domains adapting them across samples reducing the multi-source into a single-source setting. In the bottom part of the table we compare against state-of-the-art Universal DA approaches CMU [9] and DANCE [37], already introduced in the main paper, and with ROS [1], our main competitor. In all the cases, HyMOS shows very promising results demonstrating its effectiveness and versatility.

## References

DomainNet							
Multi-Source Closed Set							
	→ clp	→ inf	→ pnt	→ qdr	→ rel	→ skt	Avg.
Source Only (from [22])	52.1	23.4	47.7	13.0	60.7	46.5	40.6
LtC-MSDA [50]	63.1	28.7	56.1	16.3	66.1	53.8	47.4
DRT [22]	71.0	31.6	<b>61.0</b>	12.3	71.4	60.7	51.3
HyMOS Source Only	68.4	36.3	57.1	16.8	73.7	61.2	52.3
<b>HyMOS</b>	<b>71.5</b>	<b>41.8</b>	60.8	<b>34.5</b>	<b>74.2</b>	<b>66.6</b>	<b>58.2</b>

Multi-Source Universal									
	I,P → S			I,P → C			Avg.		
	OS*	UNK	<b>HOS</b>	OS*	UNK	<b>HOS</b>	OS*	UNK	<b>HOS</b>
CMU [9]	42.2	36.1	38.9	45.8	23.7	31.2	44.0	29.9	35.1
DANCE [37]	40.3	49.7	44.5	45.9	54.8	49.9	43.1	52.3	47.2
ROS [1]	32.6	50.7	39.7	44.5	47.7	46.0	38.6	49.2	42.9
<b>HyMOS</b>	43.7	73.0	<b>54.6</b>	45.6	76.5	<b>57.1</b>	44.7	74.8	<b>55.9</b>

Table 7: Multi-Source Closed-Set and Universal Domain Adaptation.

[4] Paola Cascante-Bonilla, Fuwen Tan, Yanjun Qi, and Vicente Ordonez. Curriculum labeling: Revisiting pseudo-labeling for semi-supervised learning. In *AAAI*, 2021.

[5] Ting Chen, Simon Kornblith, Mohammad Norouzi, and Geoffrey Hinton. A simple framework for contrastive learning of visual representations. In *ICML*, 2020.

[6] Ching-Yao Chuang, Joshua Robinson, Yen-Chen Lin, Antonio Torralba, and Stefanie Jegelka. Debiased contrastive learning. In *NeurIPS*, 2020.

[7] Gabriela Csurka. *Domain Adaptation in Computer Vision Applications*. Springer, 2017.

[8] Qianyu Feng, Guoliang Kang, Hehe Fan, and Yi Yang. Attract or distract: Exploit the margin of open set. In *ICCV*, 2019.

[9] Bo Fu, Zhangjie Cao, Mingsheng Long, and Jianmin Wang. Learning to detect open classes for universal domain adaptation. In *ECCV*, 2020.

[10] Yaroslav Ganin, Evgeniya Ustinova, Hana Ajakan, Pascal Germain, Hugo Larochelle, François Laviolette, Mario Marchand, and Victor Lempitsky. Domain-adversarial training of neural networks. *The Journal of Machine Learning Research*, 17(1):2096–2030, 2016.

[11] Rui Gong, Wen Li, Yuhua Chen, and Luc Van Gool. Dlow: Domain flow for adaptation and generalization. In *CVPR*, 2019.

[12] Kaiming He, Haoqi Fan, Yuxin Wu, Saining Xie, and Ross Girshick. Momentum contrast for unsupervised visual representation learning. In *CVPR*, 2020.

[13] Kaiming He, Xiangyu Zhang, Shaoqing Ren, and Jian Sun. Deep residual learning for image recognition. In *CVPR*, 2016.

[14] Xun Huang and Serge Belongie. Arbitrary style transfer in real-time with adaptive instance normalization. In *ICCV*, 2017.

[15] Olivier J. Hénaff, Aravind Srinivas, Jeffrey De Fauw, Ali Razavi, Carl Doersch, S. M. Ali Eslami, and Aaron van den Oord. Data-efficient image recognition with contrastive predictive coding. In *ICML*, 2020.

[16] Simon Jenni, Hailin Jin, and Paolo Favaro. Steering self-supervised feature learning beyond local pixel statistics. In *CVPR*, 2020.

[17] Prannay Khosla, Piotr Teterwak, Chen Wang, Aaron Sarna, Yonglong Tian, Phillip Isola, Aaron Maschinot, Ce Liu, and Dilip Krishnan. Supervised contrastive learning. In *NeurIPS*, 2020.

[18] Jogendra Nath Kundu, Naveen Venkat, Ambareesh Revanur, R Venkatesh Babu, et al. Towards inheritable models for open-set domain adaptation. In *CVPR*, 2020.

[19] Jogendra Nath Kundu, Rahul Mysore Venkatesh, Naveen Venkat, Ambareesh Revanur, and R. Venkatesh Babu. Class-incremental domain adaptation. In *ECCV*, 2020.

[20] Chen-Yu Lee, Tanmay Batra, Mohammad Haris Baig, and Daniel Ulbricht. Sliced wasserstein discrepancy for unsupervised domain adaptation. In *CVPR*, 2019.

[21] Yanghao Li, Naiyan Wang, Jianping Shi, Jiaying Liu, and Xiaodi Hou. Revisiting batch normalization for practical domain adaptation. In *ICLR*, 2017.

[22] Yunsheng Li, Lu Yuan, Yingpeng Chen, Pei Wang, and Nuno Vasconcelos. Dynamic transfer for multi-source domain adaptation. In *CVPR*, 2021.

[23] Hong Liu, Zhangjie Cao, Mingsheng Long, Jianmin Wang, and Qiang Yang. Separate to adapt: Open set domain adaptation via progressive separation. In *CVPR*, 2019.

[24] Mingsheng Long, Yue Cao, Jianmin Wang, and Michael I. Jordan. Learning transferable features with deep adaptation networks. In *ICML*, 2015.

[25] Mingsheng Long, ZHANGJIE CAO, Jianmin Wang, and Michael I Jordan. Conditional adversarial domain adaptation. In *NeurIPS*, 2018.

[26] Yawei Luo, Ping Liu, Tao Guan, Junqing Yu, and Yi Yang. Adversarial style mining for one-shot unsupervised domain adaptation. In *NeurIPS*, 2020.

[27] Orchid Majumder, Avinash Ravichandran, Subhransu Maji, Marzia Polito, Rahul Bhotika, and Stefano Soatto. Revisiting contrastive learning for few-shot classification. *arXiv preprint arXiv:2101.11058*, 2021.

[28] Marc Masana, Idoia Ruiz, Joan Serrat, Joost van de Weijer, and Antonio M. Lopez. Metric learning for novelty and anomaly detection. In *BMVC*, 2018.

[29] Pascal Mettes, Elise van der Pol, and Cees Snoek. Hyperspherical prototype networks. In *NeurIPS*, 2019.

[30] Yingwei Pan, Ting Yao, Yehao Li, Chong-Wah Ngo, and Tao Mei. Exploring category-agnostic clusters for open-set domain adaptation. In *CVPR*, 2020.

[31] Pau Panareda Busto and Juergen Gall. Open set domain adaptation. In *ICCV*, 2017.

[32] Xingchao Peng, Qinxun Bai, Xide Xia, Zijun Huang, Kate Saenko, and Bo Wang. Moment matching for multi-source domain adaptation. In *ICCV*, 2019.

[33] Senthil Purushwalkam and Abhinav Gupta. Demystifying contrastive self-supervised learning: Invariances, augmentations and dataset biases. In *NeurIPS*, 2020.

[34] Sayan Rakshit, Dipesh Tamboli, Pragati Shuddhodhan Meshram, Biplab Banerjee, Gemma Roig, and Subhasis Chaudhuri. Multi-source open-set deep adversarial domain adaptation. In *ECCV*, 2020.

[35] Paolo Russo, Fabio Maria Carlucci, Tatiana Tommasi, and Barbara Caputo. From source to target and back: symmetric bi-directional adaptive gan. In *CVPR*, 2018.

[36] Kate Saenko, Brian Kulis, Mario Fritz, and Trevor Darrell. Adapting visual category models to new domains. In *ECCV*, 2010.

[37] Kuniaki Saito, Donghyun Kim, Stan Sclaroff, and Kate Saenko. Universal domain adaptation through self-supervision. In *NeurIPS*, 2020.

[38] Kuniaki Saito, Shohei Yamamoto, Yoshitaka Ushiku, and Tatsuya Harada. Open set domain adaptation by backpropagation. In *ECCV*, 2018.

[39] Swami Sankaranarayanan, Yogesh Balaji, Carlos D Castillo, and Rama Chellappa. Generate to adapt: Aligning domains using generative adversarial networks. In *CVPR*, 2018.

[40] Kihyuk Sohn, David Berthelot, Nicholas Carlini, Zizhao Zhang, Han Zhang, Colin A Raffel, Ekin Dogus Cubuk, Alexey Kurakin, and Chun-Liang Li. Fixmatch: Simplifying semi-supervised learning with consistency and confidence. In *NeurIPS*, 2020.

[41] Jihoon Tack, Sangwoo Mo, Jongheon Jeong, and Jinwoo Shin. Csi: Novelty detection via contrastive learning on distributionally shifted instances. In *NeurIPS*, 2020.

[42] Yonglong Tian, Dilip Krishnan, and Phillip Isola. Contrastive multiview coding. In *ECCV*, 2020.

[43] Yonglong Tian, Chen Sun, Ben Poole, Dilip Krishnan, Cordelia Schmid, and Phillip Isola. What makes for good views for contrastive learning? In *NeurIPS*, 2020.

[44] Eric Tzeng, Judy Hoffman, Kate Saenko, and Trevor Darrell. Adversarial discriminative domain adaptation. In *CVPR*, 2017.

[45] Laurens Van der Maaten and Geoffrey Hinton. Visualizing data using t-sne. *Journal of machine learning research*, 9(11), 2008.

[46] Hemanth Venkateswara, Jose Eusebio, Shayok Chakraborty, and Sethuraman Panchanathan. Deep hashing network for unsupervised domain adaptation. In *CVPR*, 2017.

[47] Feng Wang and Huaping Liu. Understanding the behaviour of contrastive loss. In *CVPR*, 2021.

[48] Feng Wang, Xiang Xiang, Jian Cheng, and Alan Loddon Yuille. Normface: L2 hypersphere embedding for face verification. In *ACM Multimedia*, 2017.

[49] Hang Wang, Minghao Xu, Bingbing Ni, and Wenjun Zhang. Learning to combine: Knowledge aggregation for multi-source domain adaptation. In *ECCV*, 2020.

[50] Hang Wang, Minghao Xu, Bingbing Ni, and Wenjun Zhang. Learning to combine: Knowledge aggregation for multi-source domain adaptation. In *ECCV*, 2020.

[51] Tongzhou Wang and Phillip Isola. Understanding contrastive representation learning through alignment and uniformity on the hypersphere. In *ICML*, 2020.

[52] Longhui Wei, Lingxi Xie, Jianzhong He, Jianlong Chang, Xiaopeng Zhang, Wengang Zhou, Houqiang Li, and Qi Tian. Can semantic labels assist self-supervised visual representation learning? *arXiv preprint arXiv:2011.08621*, 2020.

[53] Mike Wu, Chengxu Zhuang, Milan Mosse, Daniel Yamins, and Noah Goodman. On mutual information in contrastive learning for visual representations. *arXiv preprint arXiv:2005.13149*, 2020.

- [54] Zhirong Wu, Yuanjun Xiong, Stella X. Yu, and Dahua Lin. Unsupervised feature learning via non-parametric instance discrimination. In *CVPR*, 2018.
- [55] Jiacheng Xu and Greg Durrett. Spherical latent spaces for stable variational autoencoders. In Ellen Riloff, David Chiang, Julia Hockenmaier, and Jun’ichi Tsujii, editors, *EMNLP*, 2018.
- [56] Jiaolong Xu, Liang Xiao, and Antonio Lopez. Self-supervised domain adaptation for computer vision tasks. *IEEE ACCESS*, 7:156694–156706, 2019.
- [57] Ruijia Xu, Guanbin Li, Jihan Yang, and Liang Lin. Larger norm more transferable: An adaptive feature norm approach for unsupervised domain adaptation. In *ICCV*, 2019.
- [58] Hongliang Yan, Yukang Ding, Peihua Li, Qilong Wang, Yong Xu, and Wangmeng Zuo. Mind the class weight bias: Weighted maximum mean discrepancy for unsupervised domain adaptation. In *CVPR*, 2017.
- [59] Luyu Yang, Yogesh Balaji, Ser-Nam Lim, and Abhinav Shrivastava. Curriculum manager for source selection in multi-source domain adaptation. In *ECCV*, 2020.
- [60] Yang You, Igor Gitman, and Boris Ginsburg. Large batch training of convolutional networks. *arXiv preprint arXiv:1708.03888*, 2017.
- [61] Yifan Zhang, Bryan Hooi, Dapeng Hu, Jian Liang, and Jiashi Feng. Unleashing the power of contrastive self-supervised visual models via contrast-regularized fine-tuning. *arXiv preprint arXiv:2102.06605*, 2021.